Geophysical Prospecting, 1998, **46**, 441–454

Seismic and ultrasonic velocities in permafrost[1]

José M. Carcione[2] and Géza Seriani[2]

Abstract

We calculate the compressional- and shear-wave velocities of permafrost as a function of unfrozen water content and temperature. Unlike previous theories based on simple slowness and/or moduli averaging or two-phase models, we use a Biot-type three-phase theory that considers the existence of two solids (solid and ice matrices) and a liquid (unfrozen water). The compressional velocity for unconsolidated sediments obtained with this theory is close to the velocity computed with Wood's model, since Biot's theory involves a Wood averaging of the moduli of the single constituents. Moreover, the model gives lower velocities than the well-known slowness averaging theory (Wyllie's equation). For consolidated Berea sandstone, the theory underestimates the value of the compressional velocity below 0°C. Computing the average bulk moduli by slowness averaging the ice and solid phases and Wood averaging the intermediate moduli with the liquid phase yields a fairly good fit of the experimental data. The proportion of unfrozen water and temperature are closely related. Fitting the wave velocity at a given temperature allows the prediction of the velocity at the whole range of temperatures, provided that the average pore radius and its standard deviation are known.

Introduction

Knowledge of the physical properties of frozen soils is essential for the exploitation of mineral resources in polar areas and quantification of the amount of drilling necessary for the construction of highways and pipelines. Exploration in polar regions requires the knowledge of permafrost properties, in particular the degree of freezing of the interstitial water. This has a negligible effect on density and magnetic permeability, precluding the use of gravimetric and magnetic techniques. Fortunately, freezing has a marked effect on wave velocities (Timur 1968). Hence, seismic and acoustic logging methods constitute the best way to quantify the degree of ice and water saturation. Laboratory measurements of acoustic velocities in frozen porous media have been reported by several researchers, notably Nakano, Martin and Smith (1972), King (1977) and Kurfurst (1976). All of them observed a sharp increase in velocities as the temperature was decreased below 0°C, mainly in sandstone samples.

Velocity control of near-surface frozen sediments is essential for the interpretation of seismic reflection surveys. In this sense, a suitable model relating seismic velocities to

[1] Received May 1997, revision accepted February 1998.
[2] Osservatorio Geofisico Sperimentale, PO Box 2011 Opicina, 34016 Trieste, Italy.

porosity and saturation is required. Timur (1968) proposed a three-phase time-average equation based on slowness averaging (Wyllie's equation) for modelling consolidated permafrost sediments. Moreover, he found that as the temperature decreases below 0°C, the water contained in the large pores freezes first, and that the freezing process ends between −21°C and −22°C, in accordance with the phase diagram of the sodium chloride–water system. The problem of transition from 'suspension' to 'compacted' sediment was treated with combined models. For instance, averaging bulk moduli weighted with the respective porosities (Voigt's model (Voigt 1928)) gives a simple model for consolidated sediments, while averaging the reciprocals of bulk moduli (Reuss's model (Reuss 1929)) accounts for unconsolidated media (e.g. Yin 1992). Zimmerman and King (1986) used the two-phase theory developed by Kuster and Toksöz (1974), assuming that unconsolidated permafrost can be approximated by an assemblage of spherical quartz grains embedded in a matrix composed of spherical inclusions of water and ice. They first compute the effective elastic moduli of the ice–water mixture with water playing the role of inclusion. This yields a homogeneous medium where the sand grains are the inclusions.

A three-phase theory based on first principles has been recently proposed by Leclaire, Cohen-Tĕnoudji and Aguirre-Puente (1994). The theory, hereafter called the LCA model, assumes that there is no direct contact between solid grains and ice, since, in principle, water tends to form a thin film around the grains. The theory predicts three compressional waves and two shear waves and can be applied to unconsolidated and consolidated media. Leclaire *et al.* (1994) also provide a thermodynamic relationship between the proportion of unfrozen water and temperature. In this work, we first compare Leclaire *et al.*'s (1994) model with the other theories, as a function of water saturation. We then analyse the effect of temperature on wave velocity and use the theory to fit experimental data obtained by Timur (1968) and Zimmerman and King (1986).

Phenomenological and two-phase models

Several two-phase models have been adapted for modelling the wave velocity of a three-phase medium. The basic material properties and their descriptions are listed in Appendix A. All the models assume that the constituents move together, so that the composite density is simply the volume-weighted average of the densities of the constituents, given by

$$\rho = \phi_{\rm w}\rho_{\rm w} + \phi_{\rm i}\rho_{\rm i} + \phi_{\rm s}\rho_{\rm s}, \tag{1}$$

provided that $\phi_{\rm w} + \phi_{\rm i} + \phi_{\rm s} = 1$. The compressional- and shear-wave velocities are then given by

$$V_{\rm P} = \sqrt{\frac{K + 4G/3}{\rho}}, \quad V_{\rm S} = \sqrt{\frac{G}{\rho}}, \tag{2}$$

where K is the composite bulk modulus and G is the composite shear modulus.

Voigt's model

This model is based on bulk modulus averaging (isostrain assumption). The composite moduli are given by

$$K = \phi_w K_w + \phi_i K_i + \phi_s K_s \tag{3}$$

and

$$G = \phi_i \mu_i + \phi_s \mu_s. \tag{4}$$

Reuss's model

Reuss's model (Reuss 1929), also known as Wood's model (Wood 1941), averages the reciprocal of the bulk moduli (isostress assumption). The composite bulk modulus is obtained from

$$\frac{1}{K} = \frac{\phi_w}{K_w} + \frac{\phi_i}{K_i} + \frac{\phi_s}{K_s} \tag{5}$$

and the shear modulus is obtained from

$$\frac{1}{G} = \frac{\phi_i}{\mu_i} + \frac{\phi_s}{\mu_s} \tag{6}$$

for $\phi_w = 0$ and $G = 0$ for $\phi_w \neq 0$. These equations have been proved useful for emulsions and suspensions of solid particles in a continuous liquid phase (unconsolidated sediments, see White 1965; Schön 1996).

Time-average model

Wyllie, Gregory and Gardner (1956) introduced the time-average formula, that consists of slowness averaging. The composite moduli are obtained from

$$\sqrt{\frac{\rho}{K + 4G/3}} = \phi_w \sqrt{\frac{\rho_w}{K_w}} + \phi_i \sqrt{\frac{\rho_i}{K_i + 4\mu_i/3}} + \phi_s \sqrt{\frac{\rho_s}{K_s + 4\mu_s/3}} \tag{7}$$

and

$$\sqrt{\frac{\rho}{G}} = \phi_i \sqrt{\frac{\rho_i}{\mu_i}} + \phi_s \sqrt{\frac{\rho_s}{\mu_s}} \tag{8}$$

if $\phi_w = 0$ and $G = 0$ for $\phi_w \neq 0$.

This model was applied by Timur (1968) to consolidated permafrost sediments.

Minshull et al.*'s model*

Application of Gassmann's two-phase equation (Gassmann 1951) to permafrost follows the work by Minshull, Singh and Westbrook (1994) who used the equation for

modelling partially hydrated sediments. First, the time-average relationship is used to determine the moduli K_1 and G_1 for full ice saturation,

$$\sqrt{\frac{\rho_1}{K_1+4G_1/3}}=\phi_s\sqrt{\frac{\rho_s}{K_s+4\mu_s/3}}+(1-\phi_s)\sqrt{\frac{\rho_i}{K_i+4\mu_i/3}}, \tag{9}$$

$$\sqrt{\frac{\rho_1}{G_1}}=\phi_s\sqrt{\frac{\rho_s}{\mu_s}}+(1-\phi_s)\sqrt{\frac{\rho_i}{\mu_i}}, \tag{10}$$

where $\rho_1=\phi_s\rho_s+(1-\phi_s)\rho_i$. Secondly, Gassmann's equation determines the moduli for the water-filled sediment,

$$K_2-K_{sm}=\frac{(1-K_{sm}/K_s)^2}{(1-\phi_s)/K_w+\phi_s/K_s-K_{sm}/K_s^2}, \tag{11}$$

$$G_2=\mu_{sm}, \tag{12}$$

with $\rho_2=\phi_s\rho_s+(1-\phi_s)\rho_w$.

Finally, the moduli for partial saturation are obtained by slowness averaging as

$$\sqrt{\frac{\rho}{K+4G/3}}=(1-s)\sqrt{\frac{\rho_1}{K_1+4G_1/3}}+s\sqrt{\frac{\rho_2}{K_2+4G_2/3}} \tag{13}$$

and

$$\sqrt{\frac{\rho}{G}}=(1-s)\sqrt{\frac{\rho_1}{G_1}}+s\sqrt{\frac{\rho_2}{G_2}}, \tag{14}$$

where $s=\phi_w/(1-\phi_s)$ is the water saturation.

Zimmerman and King's model

Zimmerman and King (1986) and King, Zimmerman and Corwin (1988) extended the two-phase theory developed by Kuster and Toksöz (1974) for modelling unconsolidated permafrost. They first compute the effective elastic moduli of the ice–water mixture with water playing the role of inclusion. This yields a homogeneous medium where the sand grains are the inclusions.

The moduli of the homogeneous medium are given by

$$\frac{K_h}{K_i}=\frac{1+[4\mu_i(K_w-K_i)/(3K_w+4\mu_i)K_i]s}{1-[3(K_w-K_i)/(3K_w+4\mu_i)]s} \tag{15}$$

and

$$\frac{G_h}{\mu_i}=\frac{(1-s)(9K_w+8\mu_i)}{9K_i+8\mu_i+s(6K_i+12\mu_i)}, \tag{16}$$

where $s=\phi_w/(1-\phi_s)$ is the water concentration. In the second stage, the inclusion

concentration is ϕ_s. The expressions of the elastic moduli are given by

$$\frac{K}{K_h} = \frac{1 + [4G_h(K_s - K_h)/(3K_s + 4G_h)K_h]\phi_s}{1 - [3(K_s - K_h)/(3K_s + 4G_h)]\phi_s} \tag{17}$$

and

$$\frac{G}{G_h} = \frac{(6K_h + 12G_h)\mu_s + (9K_h + 8G_h)[(1 - \phi_s)G_h + \phi_s\mu_s]}{(9K_h + 8G_h)G_h + (6K_h + 12G_h)[(1 - \phi_s)\mu_s + \phi_s G_h]}. \tag{18}$$

Three-phase model

The theory developed by Leclaire *et al.* (1994) explicitly takes into account the presence of the three phases. The three compressional velocities of the three-phase frozen porous medium are given by

$$V_{Pi} = \left[\mathrm{Re}\left(\sqrt{\Lambda_i}\right)\right]^{-1}, \quad i = 1, \ldots, 3, \tag{19}$$

where Re denotes the real part and Λ_i are obtained from the following characteristic equation:

$$A\Lambda^3 - [\rho_{11}B + \rho_{22}C + \rho_{33}D - 2(R_{11}R_{23}\rho_{23} + R_{33}R_{12}\rho_{12})]\Lambda^2$$
$$+ [bR_{11} + cR_{22} + dR_{33} - 2(\rho_{11}\rho_{23}R_{23} + \rho_{33}\rho_{12}R_{12})]\Lambda - a = 0. \tag{20}$$

The velocities of the two shear waves are given by

$$V_{Si} = \left[\mathrm{Re}\left(\sqrt{\Omega_i}\right)\right]^{-1}, \quad i = 1, 2, \tag{21}$$

where Ω_i are obtained from the second-order equation

$$\Omega^2\rho_{22}\mu_1\mu_3 - \Omega(\mu_1 b + \mu_3 d) + a = 0. \tag{22}$$

The coefficients in (20) and (22) are given in Appendix B.

Assuming a Gaussian porosimetric distribution, the unfrozen water proportion ϕ_w can be obtained as a function of temperature as

$$\phi_w = (1 - \phi_s)\Delta r^{-1}(2\pi)^{-1/2} \int_{-\infty}^{r_0/\ln(T_0/T)} \exp\left[-(r - r_{av})^2/(2\Delta r^2)\right]\mathrm{d}r, \tag{23}$$

where $r_0 = 2.28 \times 10^{-10}$ m, r_{av} is the average pore radius and Δr is the standard deviation (Leclaire *et al.* 1994). The temperature T is given in degrees Kelvin and $T_0 = 273$ °K.

Examples

The material properties for an unconsolidated porous medium are given in Table 1 and we assume a porosity $1 - \phi_s = 0.4$. The stiffnesses and densities are those given by Zimmerman and King (1986) and, for completeness, the values of the permeabilities and

Table 1. Properties of unconsolidated permafrost.

Quartz	$\rho_s = 2700$ kg/m^3	$K_s = 44$ GPa	$\mu_s = 37$ GPa	$\kappa_{s0} = 10^{-11}$ m^2
Ice	$\rho_i = 920$ kg/m^3	$K_i = 8.4$ GPa	$\mu_i = 3.7$ GPa	$\kappa_{i0} = 5 \times 10^{-4}$ m^2
Water	$\rho_w = 1000$ kg/m^3	$K_w = 2$ GPa	$\mu_w = 0$ GPa	$\bar{\eta}_w = 1.798 \times 10^{-3}$ cP
$K_{sm} = 0$ GPa	$\mu_{sm} = 0$ GPa	$r_s = 180$ μm	$r_{12} = 0.5$	$r_{23} = 0.5$

water viscosity are given, though they do not greatly affect the wave velocities at low frequencies. Figure 1 compares low-frequency compressional- and shear-wave velocities versus water saturation $\phi_w/(1-\phi_s)$, corresponding to the different theories. The curve LCA1 corresponds to the fast wave and LCA2 and LCA3 to the slow waves. These are generated by the out-of-phase motion between two of the three phases (Leclaire, Cohen-Tĕnoudji and Aguirre-Puente 1995). Note that the theory assumes that there is no direct contact between the solid substrate and ice, allowing a differential motion between the

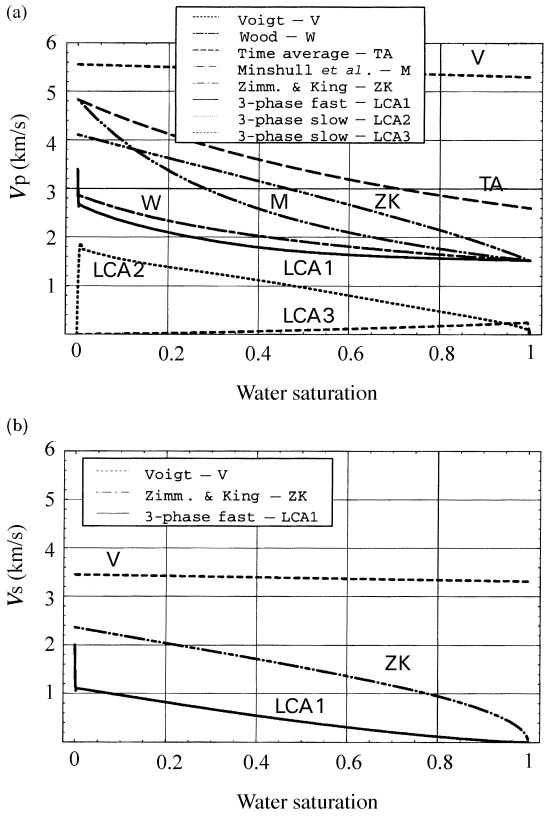

Figure 1. Low-frequency (a) compressional-wave and (b) shear-wave velocities versus the proportion of unfrozen water predicted by the different theories. The medium is unconsolidated and its properties are given in Table 1. The curves corresponding to the three-phase theory are labelled LCA, where LCA1 is the fast wave and LCA2 and LCA3 are the slow waves.

different phases. In order to obtain the curves, we have neglected the dependence of water content on temperature. Actually, as indicated by (23) and illustrated in the example below, a rigorous application of the theory implies the use of a precise thermodynamic relationship between the proportion of unfrozen water and temperature.

The curves LCA1, M (Minshull *et al.* 1994), ZK (Zimmerman and King 1986) and W (Wood's model) in Fig. 1(a) meet and give Biot's results at full water saturation, but they give different values at full ice saturation. In particular, Wood's velocity (W) is very close to the velocity predicted by the LCA theory. This can be explained from the fact that the average bulk moduli K_{av} and μ_{av} are very similar to Wood's averages. All the theories correctly predict the behaviour of the fast-wave velocity in a partially frozen medium, i.e. velocity decreases for increasing water saturation. Note that the time-average theory predicts a higher velocity than the other three theories. Moreover, we observe that the velocity given by the curve LCA1 increases abruptly approaching full ice saturation, as indicated by the nearly vertical segment of the curve. Finally, the V (Voigt's model) curve seems to overestimate the velocity.

On the other hand, the shear wave predicted by the LCA model propagates mainly through the ice skeleton (LCA1 in Fig. 1b), and gives a lower velocity than that predicted by Zimmerman and King's model (ZK). This can be explained by the fact that, in the LCA model, the ice and solid frames are not in direct contact, reducing the stiffness of the composite. Both curves yield zero velocity for full water saturation, since at this point the medium constitutes an unconsolidated mixture of sand and water.

Figure 2 shows the compressional-wave velocity versus temperature in (consolidated) Berea sandstone. The dots correspond to experimental data measured by Timur (1968), with the sample subjected to a uniaxial pressure of 313 atm and the pore fluid under atmospheric pressure. The sample, with a porosity equal to 0.2, was first cooled to -23°C, and then brought back to room temperature. Two curves, computed at 200 kHz, are fitted to the experimental points. The properties, illustrated in Table 2, are taken from Timur (1968) and Winkler (1985), assuming $r_{av} = 10\,\mu$m and $\Delta r = 4\,\mu$m. The dotted curve corresponds exactly to the LCA theory. As can be seen the velocity is underestimated below 0°C. The broken line, which fits the data fairly well, was obtained from the three-phase model by computing the average bulk moduli as follows:

$$K_{av} = \left(\frac{1 - \phi_w}{K'} + \frac{\phi_w}{K_w} \right)^{-1} \tag{24}$$

and

$$\mu_{av} = \left(\frac{1 - \phi_w}{\mu'} + \frac{\phi_w}{2\omega\eta_w} \right)^{-1}, \tag{25}$$

where

$$K' = \frac{\phi_s \rho_s + \phi_i \rho_i}{\phi_s + \phi_i} \left(V_P'^2 - \frac{4}{3} V_S'^2 \right), \tag{26}$$

$$\mu' = \frac{\phi_s \rho_s + \phi_i \rho_i}{\phi_s + \phi_i} V_S'^2, \tag{27}$$

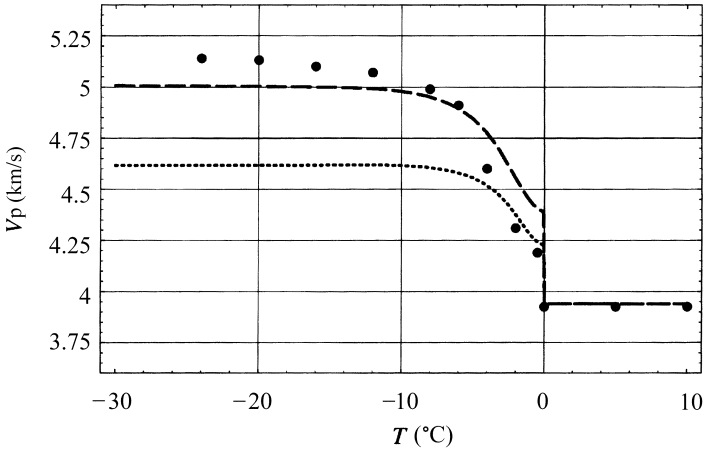

Figure 2. Compressional-wave velocity versus temperature in (consolidated) Berea sandstone at 200 kHz. The dots correspond to experimental data measured by Timur (1968). The dotted curve corresponds exactly to the three-phase theory. The broken line, which fits the data fairly well, was obtained from a modification of this model.

$$V'_{\rm P} = \left\{ \frac{\phi_{\rm s}}{\phi_{\rm s}+\phi_{\rm i}} \left[\frac{1}{\rho_{\rm s}} \left(\frac{K_{\rm s}}{1-c_1} + \left(\frac{4}{3}\right) \frac{\mu_{\rm s}}{1-g_1} \right) \right]^{-1/2} \right.$$
$$\left. + \frac{\phi_{\rm i}}{\phi_{\rm s}+\phi_{\rm i}} \left[\frac{1}{\rho_{\rm i}} \left(\frac{K_{\rm i}}{1-c_3} + \left(\frac{4}{3}\right) \frac{\mu_{\rm i}}{1-g_3} \right) \right]^{-1/2} \right\}^{-1} \tag{28}$$

and

$$V'_{\rm S} = \left\{ \frac{\phi_{\rm s}}{\phi_{\rm s}+\phi_{\rm i}} \left[\left(\frac{1}{\rho_{\rm s}}\right) \frac{\mu_{\rm s}}{1-g_1} \right]^{-1/2} + \frac{\phi_{\rm i}}{\phi_{\rm s}+\phi_{\rm i}} \left[\left(\frac{1}{\rho_{\rm i}}\right) \frac{\mu_{\rm i}}{1-g_3} \right]^{-1/2} \right\}^{-1}. \tag{29}$$

Leclaire *et al.* (1994) computed the average moduli by extending Biot's equations to include the ice phase. This generalization involves a Wood averaging. In (24)–(29), we use a time-average equation for computing the moduli of a solid-ice effective frame. These moduli are then Wood averaged together with the water modulus for obtaining $K_{\rm av}$ and $\mu_{\rm av}$. In fact, computing the average bulk moduli in this way increases the value of the compressional velocity and the theory better fits Timur's (1968) experimental values below 0°C. Moreover, the sharp velocity increase at 0°C, observed in the

Table 2. Properties of partially frozen Berea sandstone.

Quartz	$\rho_{\rm s}$ = 2650 kg/m^3	$K_{\rm s}$ = 38.7 GPa	$\mu_{\rm s}$ = 39.6 GPa	$\kappa_{\rm s0} = 1.07\ 10^{-13}$ m^2
Ice	$\rho_{\rm i}$ = 920 kg/m^3	$K_{\rm i}$ = 8.58 GPa	$\mu_{\rm i}$ = 3.32 GPa	$\kappa_{\rm i0} = 5 \times 10^{-4}$ m^2
Water	$\rho_{\rm w}$ = 1000 kg/m^3	$K_{\rm w}$ = 2.25 GPa	$\mu_{\rm w}$ = 0 GPa	$\bar{\eta}_{\rm w} = 1.798 \times 10^{-3}$ cP
$K_{\rm sm}$ = 14.4 GPa	$\mu_{\rm sm}$ = 13.1 GPa	$r_{\rm s}$ = 50 μm	r_{12} = 0.5	r_{23} = 0.5

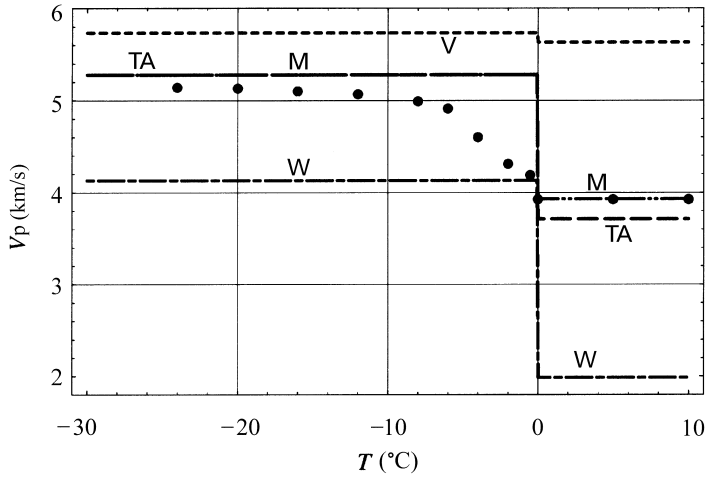

Figure 3. Compressional-wave velocity versus temperature in (consolidated) Berea sandstone. The dots correspond to experimental data measured by Timur (1968) and the other curves to the different phenomenological theories. These can be identified in the legend provided in Fig. 1(a).

experiments, is a feature that theory predicts fairly well. This modification to the original theory could be considered a cementation effect, where ice forms at grain contacts and increases the stiffness of the matrix (e.g. Jacoby, Dvorkin and Liu 1996).

Figure 3 shows Timur's (1968) experimental points for Berea sandstone, compared with the phenomenological theories. As suggested by Zimmerman and King (1986), their model, which works well for unconsolidated permafrost, cannot be directly applied to consolidated permafrost; consequently, the predictions of (17) and (18) are not shown in Fig. 3. Since the models do not consider the temperature dependence, we have assumed that below freezing point, the pores are fully saturated with ice, and that above freezing point the pores are water saturated. As can be appreciated, the best fit is obtained with Minshull *et al.*'s (1994) model (M). Note that below 0°C the time-average curve coincides with the M curve.

Finally, Fig. 4 shows compressional velocity versus temperature, where we attempted to fit the experimental velocity values corresponding to samples C2 and C5 of Zimmerman and King (1986), which have a porosity of 0.4. The samples were measured at 660 kHz, at a hydrostatic confining stress of 0.35 MPa and at a temperature of approximately −5°C. As in Fig. 2, the dotted line corresponds to Leclaire *et al.*'s (1994) theory and the broken line to the modified three-phase model. For the calculation, we have assumed that the porosimetric distribution has an average radius of $r_{av} = 30\,\mu$m and a standard deviation $\Delta r = 10\,\mu$m. Figure 5 shows the proportion of unfrozen water ϕ_w as a function of temperature, computed from (23). The temperature −5°C corresponds to an unfrozen water content of 2.2×10^{-6}, in contrast to the values, ranging between 0.09 and 0.17, predicted by Zimmerman and

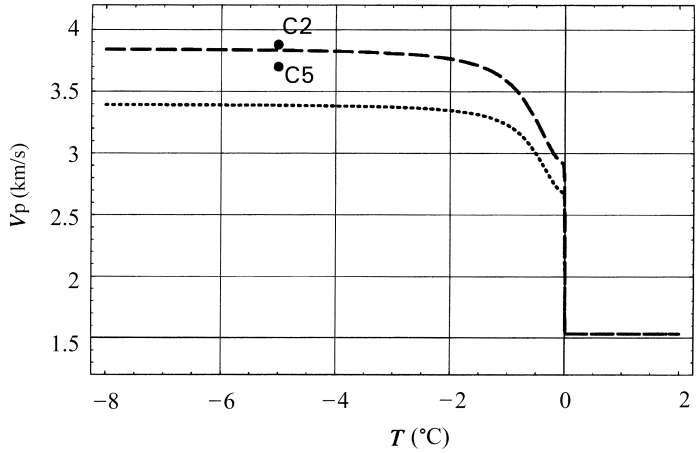

Figure 4. Compressional-wave velocity versus temperature, where we attempted to fit the experimental velocity values corresponding to samples C2 and C5 of Zimmerman and King (1986).

King (1986). This discrepancy could be due to the fact that (23) holds for fresh water. To overcome this limitation, the quantity r_0 can be used as a parameter in order to take into account the salinity content of the pore water. As stated by Timur (1968), as the ice crystallizes out as pure H_2O, the sodium chloride concentration of the remaining solution increases, thereby further lowering the freezing point. Hence, ice may be thought of as forming on the walls of the larger pores and growing into the pore spaces.

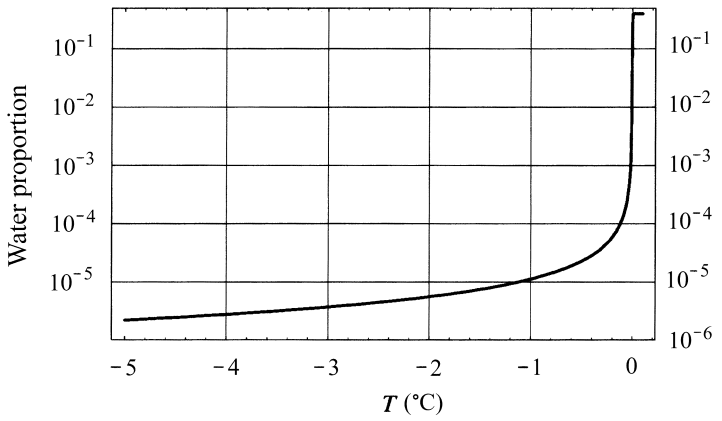

Figure 5. Proportion of unfrozen water versus temperature for an average pore radius of $r_{av} = 30\,\mu$m and a standard deviation $\Delta r = 10\,\mu$m.

Conclusions

Leclaire *et al.*'s (1994) three-phase theory is used for computing the wave velocity of consolidated and unconsolidated permafrost. The model describes the phase transition of the interstitial fluid between liquid state and solid state.

In principle, the predictions of the theory as a function of the proportion of unfrozen water are close to the predictions of Wood's (1941) model. However, fitting the velocities for consolidated permafrost at different temperatures requires a slowness averaging of the ice and solid phases when computing the average moduli. This phenomenological modification of the theory, probably simulating grain cementation, gives higher dilatational and shear moduli and could be implemented from first principles by including the crossed terms (neglected in the theory) that are responsible for the direct mechanical contact between the ice and solid phases.

Differences between the theoretical velocity and the experimental data may be due to several factors not considered by the theory, for instance the presence of clay, water salinity, dependence of the solid and ice moduli on temperature and cementation between the grains. The influence of these factors will be investigated in future work.

Acknowledgements

We thank Norsk Hydro a.s. (Bergen) for financing the research, and Professor F. Cohen-Tënoudji for providing a copy of Dr Leclaire's thesis.

Appendix A

List of symbols

ϕ_s	proportion of solid;
ϕ_w	proportion of unfrozen water;
ϕ_i	proportion of ice;
ρ_s	solid density;
ρ_w	water density;
ρ_i	ice density;
K_s	solid bulk modulus;
K_w	water bulk modulus;
K_i	ice bulk modulus;
K_{sm}	bulk modulus of the matrix formed by the solid phase;
K_{max}	Kuster–Toksöz's bulk modulus;
K_{im}	bulk modulus of the matrix formed by the ice: $K_{max}[\phi_i/(1-\phi_s)]^{3.8}$;
c_1	consolidation coefficient for the solid: $K_{sm}/\phi_s K_s$;
c_3	consolidation coefficient for the ice: $K_{im}/\phi_i K_i$;
K_{av}	average bulk modulus: $[(1-c_1)\phi_s/K_s + \phi_w/K_w + (1-c_3)\phi_i/K_i]^{-1}$;
μ_s	solid shear modulus;
μ_i	ice shear modulus;

μ_{sm}	shear modulus of the matrix formed by the solid phase;
μ_{max}	Kuster–Toksöz's shear modulus;
μ_{im}	shear modulus of the matrix formed by the ice: $\mu_{max}\ [\phi_i/(1-\phi_s)]^{3.8}$;
κ_{s0}	solid matrix permeability;
κ_{i0}	ice matrix permeability;
ω	angular frequency: $2\pi f$;
T	water temperature in degrees Celsius;
$\bar{\eta}_w$	viscosity of free water: $1.798\ 10^{-3}$ exp $(-0.03753T)$ (MKS units);
h	average thickness of the unfrozen water layer: $r_s[(1+\phi_w/\phi_s)^{1/3}-1]$;
η_w	viscosity of interstitial water: $\bar{\eta}_w\ (450+h)/h$, with h in angstroms;
χ	: $(h/2)\ (\omega\rho_w/\eta_w)^{1/2}$;
Re[F(χ)]	: $1+(1/0.7178)$ exp $[0.7178(\chi-3.2)]/12$, if $\chi \leq 3.2$;
Re[F(χ)]	: $0.5+\{2\ \chi+\exp\ [-0.7178\ (\chi-3.2)]\}/12$, if $\chi > 3.2$;
Im[F(χ)]	: $\chi/6$;
η_D	dynamical viscosity of interstitial water: $\eta_w\ F(\chi)$;
g_1	consolidation coefficient for the solid: $\mu_{sm}/\phi_s\mu_s$;
g_3	consolidation coefficient for the ice: $\mu_{im}/\phi_i\mu_i$;
μ_{av}	average shear modulus: $[(\ 1-g_1)\phi_s/\mu_s+\phi_w/2\omega\eta_w+(1-g_3)\phi_i/\mu_i]^{-1}$;
r_{12}	geometrical aspect of the boundary separating solid from water;
r_{23}	geometrical aspect of the boundary separating ice from water;
r_s	average radius of solid grains;
r_{av}	average radius of the capillary pore;
Δr	standard deviation of the capillary pore.

Appendix B

Coefficients for the three-phase model

Additional expressions, corresponding to equations (20) and (22), are given below.

$$A = R_{11}R_{22}R_{33} - R_{23}^2R_{11} - R_{12}^2R_{33};$$

$$B = R_{22}R_{33} - R_{23}^2;$$

$$C = R_{11}R_{33};$$

$$D = R_{11}R_{22} - R_{12}^2;$$

$$a = \rho_{11}\rho_{22}\rho_{33} - \rho_{23}^2\rho_{11} - \rho_{12}^2\rho_{33};$$

$$b = \rho_{22}\rho_{33} - \rho_{23}^2;$$

$$c = \rho_{11}\rho_{33};$$

$$d = \rho_{11}\rho_{22} - \rho_{12}^2;$$

$$R_{11} = [(1 - c_1)\phi_s]^2 K_{av} + K_{sm} + \frac{4}{3}\{[(1 - g_1)\phi_s]^2 \mu_{av} + \mu_{sm}\};$$

$$R_{12} = [(1 - c_1)\phi_s]\phi_w K_{av};$$

$$R_{22} = \phi_w^2 K_{av};$$

$$R_{23} = [(1 - c_3)\phi_i]\phi_w K_{av};$$

$$R_{33} = [(1 - c_3)\phi_i]^2 K_{av} + K_{im} + \frac{4}{3}\{[(1 - g_3)\phi_i]^2 \mu_{av} + \mu_{im}\};$$

$$\rho_{11} = \phi_s\rho_s + (a_{12} - 1)\phi_w\rho_w - \imath b_1/\omega;$$

$$\rho_{12} = -(a_{12} - 1)\phi_w\rho_w + \imath b_1/\omega;$$

$$\rho_{22} = (a_{12} + a_{23} - 1)\phi_w\rho_w - \imath(b_1 + b_3)/\omega;$$

$$\rho_{23} = -(a_{23} - 1)\phi_w\rho_w + \imath b_3/\omega;$$

$$\rho_{33} = \phi_i\rho_i + (a_{23} - 1)\phi_w\rho_w - \imath b_3/\omega;$$

$$b_1 = \eta_D\phi_w^2/\kappa_s;$$

$$b_3 = \eta_D\phi_w^2/\kappa_i;$$

$$\kappa_s = \kappa_{s0}\phi_w^3/(1 - \phi_s)^3;$$

$$\kappa_i = \kappa_{i0}[(1 - \phi_s)/\phi_i]^2(\phi_w/\phi_s)^3;$$

$$a_{12} = r_{12}(\phi_s\rho)/(\phi_w\rho_w) + 1;$$

$$a_{23} = r_{23}(\phi_i\rho')/(\phi_w\rho_w) + 1;$$

$$\rho = (\phi_w\rho_w + \phi_i\rho_i)/(\phi_w + \phi_i);$$

$$\rho' = (\phi_w\rho_w + \phi_s\rho_s)/(\phi_w + \phi_s);$$

$$\mu_1 = [(1 - g_1)\phi_s]^2\mu_{av} + \mu_{sm};$$

$$\mu_3 = [(1 - g_3)\phi_i]^2\mu_{av} + \mu_{im}.$$

The expressions for K_{max} and μ_{max} can be found in Zimmerman and King (1986) (equations (1) and (2), respectively), with the subscript m corresponding to ice,

subscript i corresponding to air and the concentration c equal to ϕ_s. They are the moduli of the ice matrix, with the water totally frozen and the solid replaced by air.

References

Gassmann F. 1951. Über die Elastizität poröser Mediem. *Vierteljahrsschr. Naturforsch. Ges. Zürich* **96**, 1–23.

Jacoby M., Dvorkin J. and Liu X. 1996. Elasticity of partially saturated frozen sand. *Geophysics* **61**, 288–293.

King M.S. 1977. Acoustic velocities and electrical properties of frozen sandstones and shales. *Canadian Journal of Earth Sciences* **14**, 1004–1013.

King M.S., Zimmerman R.W. and Corwin R.F. 1988. Seismic and electrical properties of unconsolidated permafrost. *Geophysical Prospecting* **36**, 349–364.

Kurfurst P.J. 1976. Ultrasonic wave measurements on frozen soils at permafrost temperatures. *Canadian Journal of Earth Sciences* **13**, 1571–1576.

Kuster G.T. and Toksöz M.N. 1974. Velocity and attenuation of seismic waves in two-phase media: Part I. Theoretical formulations. *Geophysics* **51**, 1285–1290.

Leclaire Ph., Cohen-Tĕnoudji F. and Aguirre-Puente J. 1994. Extension of Biot's theory of wave propagation to frozen porous media. *Journal of the Acoustical Society of America* **96**, 3753–3768.

Leclaire Ph., Cohen-Tĕnoudji F. and Aguirre-Puente J. 1995. Observation of two longitudinal and two transverse waves in a frozen porous medium. *Journal of the Acoustical Society of America* **97**, 2052–2055.

Minshull T.A., Singh S.C. and Westbrook G.K. 1994. Seismic velocity structure at a gas hydrate reflector offshore western Colombia, from full waveform inversion. *Journal of Geophysical Research* **99**, 4715–4734.

Nakano Y., Martin R.J., III and Smith M. 1972. Ultrasonic velocities of the dilatational and shear waves in frozen soils. *Water Resources Research* **8**, 1024–1030.

Reuss A. 1929. Berechnung der Fleissgrenze von Mischkristalen auf Grund der Plastizitats belingung für EinKristalle. *Z. Angew. Math. Mech.* **9**, 49–58.

Schön J.H. 1996. *Physical Properties of Rocks. Fundamentals and Principles of Petrophysics*. Pergamon Press, Inc.

Timur A. 1968. Velocity of compressional waves in porous media at permafrost temperatures. *Geophysics* **33**, 584–595.

Voigt W. 1928. *Lehrbuch der Kristallphysik*. B. G. Terbner, Leipzig.

White J.E. 1965. *Seismic Waves, Radiation, Transmission and Attenuation*. McGraw–Hill Book Co.

Winkler K.W. 1985. Dispersion analysis of velocity and attenuation in Berea sandstone. *Journal of Geophysical Research* **90**, 6793–6800.

Wood A.B. 1941. *A Textbook of Sound*. G. Bell & Sons, Ltd, London.

Wyllie M.R.J., Gregory A.R. and Gardner L.W. 1956. Elastic wave velocities in heterogeneous porous media. *Geophysics* **21**, 41–70.

Yin H. 1992. *Acoustic velocity and attenuation of rocks: isotropy, intrinsic anisotropy, and stress induced anisotropy*. PhD dissertation, Stanford University.

Zimmerman R.W. and King M.S. 1986. The effect of the extent of freezing on seismic velocities in unconsolidated permafrost. *Geophysics* **39**, 587–606.